has not been highly purified with respect to zirconium.

Note Added in Proof.—Since this article was prepared, there has come to my attention the careful work of Graham[5] and co-workers on the isotopic constitution of germanium. These workers found that, with the exception of one sample, germanium from various ores was isotopically indistinguishable. Their averaged results for the isotopic constitution of six germanium ores, excluding the anomalous sample, can be brought into total agreement with results given here (except at mass 73 where the residual discrepancy is 0.25 percent of the abundance quoted) by application of a factor which reduces their abundances for heavier isotopes relative to the lighter, which is linear with mass, and which amounts to 0.24 percent per mass unit. This factor in all probability represents the relative discrimination of the two mass spectrometers involved. An attempt has been made to detect mass discrimination in this mass region in the Berkeley instrument by comparing measurements on atmospheric xenon with those of Nier,[3] which latter have been corrected for spectrometer discrimination. Agreement was such as to indicate that the mass discrimination of the Berkeley instrument is less than 0.025 percent per mass unit at mass 130.

[5] Graham, Macnamara, Crocker, and MacFarlane, Can. J. Chem. **29**, 89 (1951).

PHYSICAL REVIEW VOLUME 90, NUMBER 6 JUNE 15, 1953

The Angular Distribution of $Li^6(n,\alpha)H^3$ for Neutrons of 200, 270, 400, and 600 kev*

LILLIAN E. DARLINGTON, JACK HAUGSNES, HARRY M. MANN, AND JAMES H. ROBERTS
Department of Physics, Northwestern University, Evanston, Illinois

(Received March 9, 1953)

The angular distribution of $Li^6(n,\alpha)H^3$ has been measured for neutron energies of 200, 270, 400, and 600 kev by determining the distribution of triton tracks from this reaction in Ilford *C*2 plates loaded with enriched Li^6. The results fit a series of the type $A+B\cos\phi_0+C\cos^2\phi_0$, where ϕ_0 is the neutron-triton angle in the center-of-mass system. This indicates that the *s* and *p* components of the incident neutron wave predominate in the interaction.

(1) INTRODUCTION

THERE are two reasons why an investigation of $Li^6(n,\alpha)H^3$ was undertaken. (1) The use of this reaction to study neutron spectra[1] requires that the differential cross section be known as a function of neutron energy. (2) Basic data of theoretical importance can be obtained.[2] Preliminary results have been reported.[3]

The technique used is to expose Ilford *C*2 plates loaded with enriched Li^6 to unidirectional monoergic neutrons from an electrostatic generator and to measure the distribution of tracks as a function of the neutron-triton angle. Further measurements are now in progress to determine the absolute differential cross section of the reaction for neutron energies from 100 to 2000 kev. These results will be published at a later date.

(2) PLATE EXPOSURE AND PROCESSING

The 100-micron Ilford *C*2 plates loaded with enriched Li^6 were exposed to neutrons from $Li^7(p,n)$ at the electrostatic generator of the Argonne National Laboratory. The exposure geometry is shown in Fig. 1. Each plate was inside a cadmium box during exposure to shield it from the thermal neutron background. Integrated neutron fluxes of approximately 10^9 neutrons/cm^2 were used except for the exposure at 270 kev at the peak of the resonance where approximately 10^8 neutrons/cm^2 were used. All lithium targets were about 30 kev thick. The proton energy was selected so that the neutron groups would peak at 200, 270 kev, etc.

The plates were stored for at least two weeks and then given additional latent-image fading for 24 hours in an atmosphere saturated with water vapor at 22°C. The plates were processed by the technique outlined by Keepin in University of California Radiation Laboratory Report UCRL 790 (unpublished). Some of the plates were also treated with glycerine so as to be

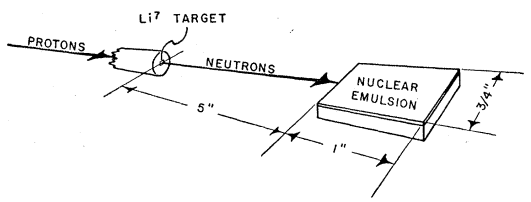

FIG. 1. Exposure geometry for Li^6 loaded plates. Each plate was inside a Cd box to shield it from the thermal neutron background due to room scattering.

* Work supported by the U. S. Atomic Energy Commission.

[1] G. R. Keepin, Jr., and J. H. Roberts, Phys. Rev. **76**, 154 (1949); Rev. Sci. Instr. **21**, 163 (1950).

[2] M. Peshkin and A. Siegert, Phys. Rev. **87**, 735 (1952); W. Solano and J. Roberts, Phys. Rev. **89**, 892 (1953).

[3] Roberts, Darlington, and Haugsnes, Phys. Rev. **82**, 299 (1951); J. Roberts and H. Mann, Phys. Rev. **83**, 202 (1951).

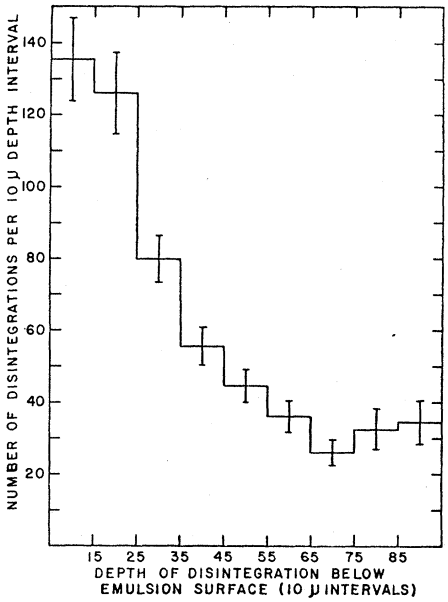

FIG. 2. Distribution of Li^6 atoms with depth below the top emulsion surface. To obtain this plot 979 tracks were measured. The vertical projection of the tritons was $\leqslant 20\mu$ in a glycerine treated plate. Corrections were made for the probability that a track would go through either emulsion surface. A curve of this type was determined for each plate; all were similar to this one.

restored approximately to their original thickness at the time of exposure.[4]

(3) TRACK MEASUREMENTS

All tracks were measured by use of Leitz Ortholux and Bausch and Lomb model CTB microscopes. 2-mm 90× apochromatic oil immersion objectives were used throughout. A protractor scale was attached to one eyepiece for the measurement of angles. Observers were trained as outlined in a previous report.[5]

For each track the following quantities were measured: the vertical projection of the alpha and triton tracks; the horizontal projection of the triton track, the alpha-track, the neutron-triton angle, and the neutron-alpha-angle. As the measurements progressed it was observed that the distribution of Li^6 atoms with depth was not uniform; measurements were therefore made of this distribution. (See Fig. 2.)

Some tracks were difficult if not impossible to interpret correctly. In such cases the observer made the most reasonable interpretation. If a track was misinterpreted this could frequently be determined from its total length, assuming it was produced by a neutron of full energy coming directly from the lithium target of the electrostatic generator. The observers were given a rough guide as an aid for such tracks. If the triton was obviously placed at the wrong end of the track the neutron-triton angle was reflected through 180°. This introduced some random error and loss in angular resolution because of scattering of the alpha and triton particles in the emulsion.

(4) CORRECTIONS FOR GEOMETRICAL SELECTION CRITERIA

The plates were scanned parallel to the direction of neutron incidence. Any track projecting into the field of view was not measured if its point of disintegration was outside the width of the scanning path. This was to prevent the selection of tracks between two scanning paths in such a way as to favor tracks making a large angle with the neutron direction.

Since the emulsion thickness was of the same order of magnitude as the track lengths, the probability that a track would go through the emulsion surface and thus be rejected was appreciable. Also, since steeply diving tracks were difficult to interpret, it was expedient to put an upper limit δ (35 microns in a 100-micron plate) on the vertical projection of an acceptable triton track. These considerations made it necessary to correct the data to what one would obtain if all tracks in a 4π solid angle had been measured.[6] In order to simplify these corrections a minimum distance from the emulsion surfaces to either end of the triton track was imposed. This distance (15 microns in a 100-micron plate) was such that the alpha-track of an otherwise acceptable disintegration could not go out of the emulsion. This minimum distance defines "effective emulsion surfaces" inside of which all parts of acceptable triton tracks must lie.

From the data we find the triton range R_T, the alpha-range R_α, and the neutron-triton angle ϕ in the laboratory system for every track. We also have a histogram giving the distribution of Li^6 atoms with depth below the emulsion surface. Let $W(\gamma)d\gamma$ = the probability that a disintegration will occur at a height between γ

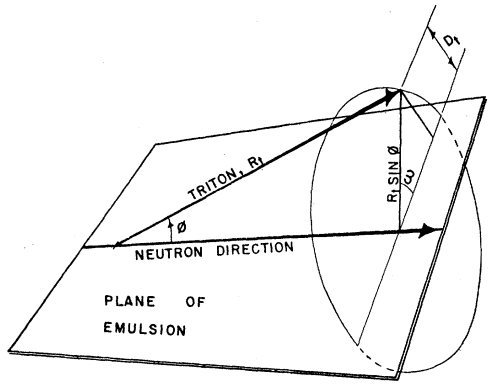

FIG. 3. The orientation of a typical triton track with respect to the emulsion plane and the direction of the incident neutrons. D_T is the vertical projection of the triton track.

[4] Details of this treatment are discussed in a separate paper to be published in the Review of Scientific Instruments.

[5] J. Haugsnes and J. H. Roberts, Los Alamos Report LA-1303, 1951 (unpublished).

[6] For a more complete discussion see G. R. Keepin and A. J. Siegert, Los Alamos Report 937, 1949 (unpublished).

and $\gamma+d\gamma$ above the lower effective emulsion surface. This function was obtained by drawing a smooth curve through the depth distribution histogram of Li^6 atoms (Fig. 2). Any azimuth ω (Fig. 3) is equally probable because of symmetry around the neutron direction. Then $W(\gamma)d\gamma d\omega/2\pi$ is the probability that a given disintegration will lie in the interval γ to $\gamma+d\gamma$, and ω to $\omega+d\omega$. The integral of this probability over all values of ω and γ compatible with the selection criteria will give the probability that the track will be accepted for measurement. This probability is given by

$$P(R_T,\phi)=\frac{1}{\pi}\int_0^{\omega_0} d\omega\left[\int_0^{a-R_T\sin\phi\sin\omega} W(\gamma)d\gamma + \int_{R_T\sin\phi\sin\omega}^{a} W(\gamma)d\gamma\right], \quad (1)$$

where a is the distance from the lower effective emulsion surface to the upper, and $\omega_0=\pi/2$ if $R_T\sin\phi\leqslant\delta$, and $\omega_0=\arcsin(\delta/R_T\sin\phi)$ if $R_T\sin\phi>\delta$.

Now $R_T=R_T(\phi,E_n)$. From the neutron energy E_n, $Q=4.78$ Mev for $Li^6(n,\alpha)$, and the range-energy curve for tritons in $C2$ emulsions, we can obtain an expression $P(\phi,E_n)$ from $P(\phi,R_T)$. $P^{-1}(\phi,E_n)$ for a typical plate is shown in Fig. 4. Each track was given a statistical weight $P^{-1}(\phi,E_n)$.

(5) DATA AND RESULTS

Table I gives the number of tracks measured on each plate and the neutron energy to which it was exposed. The total track length, $R_\alpha+R_T$, and the angle ϕ between the neutron and the triton were calculated for each track. The tracks were divided into ϕ_0 intervals, usually 15° (ϕ_0 is the neutron-triton angle in the center-of-mass system). Figure 5 shows typical histograms of the number of tracks as a function of $R_\alpha+R_T$ for some of these intervals. The triangle in each group shows where the track distribution should peak on the basis of $Q=4.78$ Mev for $Li^6(n,\alpha)$ and the Ilford range-energy curves. The "satellite" peaks appearing in some of the groups result from tracks for which the point of disintegration has been misinterpreted and from the background of epithermal neutrons. The epithermal background was estimated by calculating[7] the alpha-triton

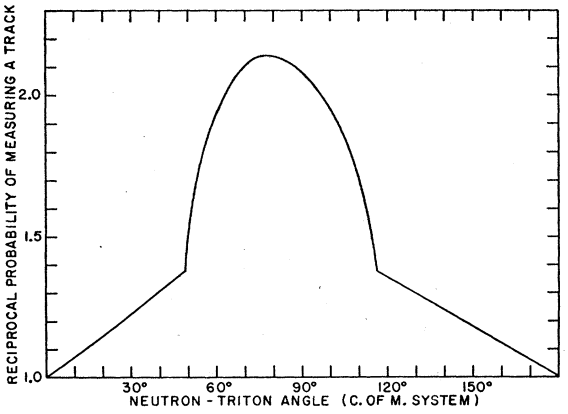

FIG. 4. Chart for determining $P^{-1}(\phi,E_n)$ for each track. This particular plot is for $E_n=600$ kev for plates 8 and 9 (see Table I).

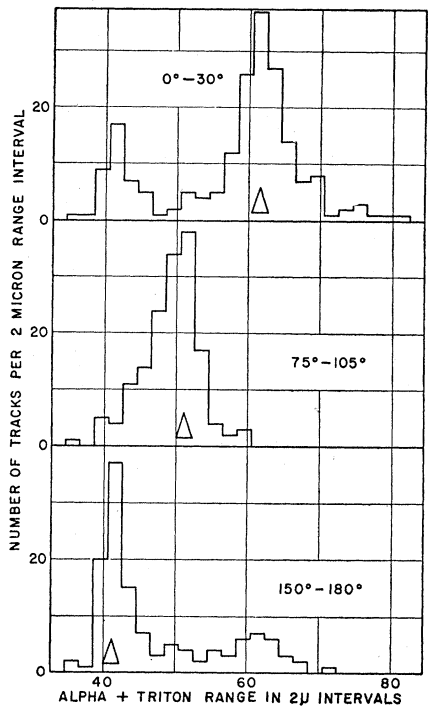

FIG. 5. Typical histograms of tracks in a few ϕ_0 intervals for $E_n=600$ kev. The arrow indicates the expected position of the peak on the basis of $Q=4.78$ Mev for $Li^6(n,\alpha)$, and the Ilford range-energy curves.

TABLE I. Tracks measured and differential cross-section coefficients.

Neutron energy (kev)	Plate number	Observer	No. of tracks measured	Capture[a] cross section (barns/atom of Li^6)	Differential capture cross-section coefficients (barns/steradian) A	B	C
200[b]	1-S	3	1000	2.1	0.10	0.08	0.18
200	2	1	948	2.1	0.09	0.11	0.23
200	3	3	996	2.1	0.08	0.14	0.26
270[b,c]	4	—	—	3.0	0.17	0.060	0.22
270	5	13	988	3.0	0.17	0.065	0.21
270	5	9	650	3.0			
400	6	3	438	1.2	0.06	0.040	0.11
400	7	1	1005	1.2	0.065	0.047	0.09
600[b]	8-S	21	1097	0.5	0.031	0.007	0.024
600	8	3	786	0.5	0.029	0.017	0.032
600	9	7	595	0.5	0.032	0.012	0.023

[a] From data of Blair and Holland (reference 8).
[b] Data from glycerine-treated plates.
[c] See 2nd paper, reference 2.

[7] M. L. Boas, Rev. Sci. Instr. (to be published).

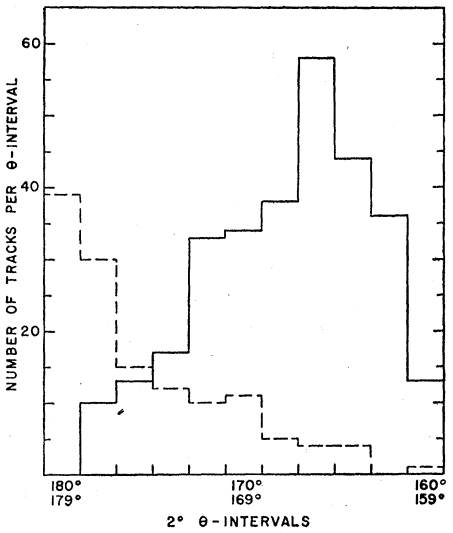

FIG. 6. Distribution of tracks as a function of the alpha-triton angle θ. The solid curve is for tracks in the interval $60°\leqslant\phi_0\leqslant120°$ for $E_n=600$ kev in plate 8-S. (See Table I.) The broken curve is for tracks in a glycerine treated plate exposed to thermal neutrons.

angle θ for tracks in the region $60°\leqslant\phi_0\leqslant120°$ in glycerine treated plates. A plot of the number of tracks per two-degree θ-interval as a function of θ for $E_n=600$ kev is shown in Fig. 6. The distribution in θ for tracks obtained from a glycerine treated plate exposed to thermal neutrons is shown in the broken histogram in the same figure. Since this latter distribution peaks $\sim\theta=180°$, and since the distribution for $E_n=600$ kev shows no rise in this region, the epithermal background must be low. Also, since the angular distribution at $E_n=400$ and 600 kev was similar to that at $E_n=270$ kev, any small number of unresolved tracks resulting from a neutron background in the vicinity of this resonance would introduce a very small correction. All background corrections would be somewhat less than the statistical accuracy of the data; therefore no such corrections were made.

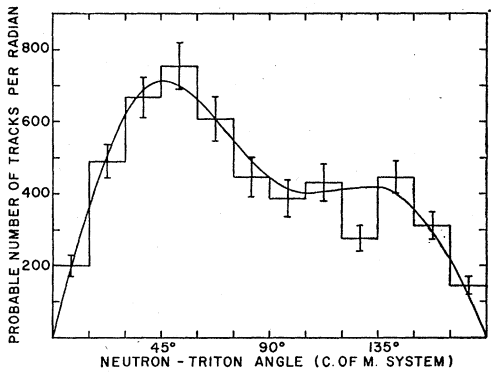

FIG. 7. Histogram showing distribution of tracks per 15° ϕ_0 interval for $E_n=200$ kev from plate 1-S (see Table I) corrected for geometrical selection criteria. The smooth curve is a plot of $2\pi Y(E_n,\phi_0)\sin\phi_0$, where $Y(E_n,\phi_0)$ is defined in Eq. (2).

The tracks in the "satellite" peaks were reflected through 180° in the laboratory system. However, these reflections proved to be of such a nature (i.e., random), that the effect was again somewhat less than the statistical accuracy of the data. The main effect of these misinterpretations was to decrease the angular resolution because of scattering of the tracks in the plate.

Each track was weighted with the factor $P^{-1}(\phi,E_n)$ as discussed in Sec. 4. A plot of $\Sigma P^{-1}(\phi,E_n)$ for all tracks in each 15°ϕ_0 interval in the c.m. system as a function of ϕ_0 for $E_n=200$ kev is shown in Fig. 7. The data for each E_n as obtained by each observer are given in Table II. The observer agreement is seen to be reasonably satisfactory in most cases. Since the observers had received more experience and more complete instruction by the time the tracks were measured in the glycerine treated plates, it is probable that these data are the most reliable. The over-all correctness of the method of analyzing the data was checked by determining the angular distribution for collimated

TABLE II. ΣP^{-1} for tracks in 15° intervals.[a]

Neutron energy (kev)	Plate number	Observer	Neutron-triton angle interval 0–15°	15°–30°	30°–45°	45°–60°	60°–75°	75°–90°	90°–105°	105°–120°	120°–135°	135°–150°	150°–165°	165°–180°	Actual ΣP^{-1} 0–180°
200[b]	1-S	3	39	95	129	146	118	86	75	84	54	86	60	28	1355
200	2	1	45	124	154	140	90	105	50	85	53	67	70	21	1325
200	3	3	56	156	159	141	110	114	49	30	42	62	57	25	1315
270	5	13	34	103	150	112	113	106	77	73	79	84	45	25	1417
270	5	9	35	90	118	143	174	83	73	76	82	64	42	18	975
400	6	3	52	103	112	132	103	129	56	72	72	79	60	31	619
400	7	1	54	88	128	125	150	130	76	28	41	84	59	36	1560
600[b]	8-S	21	23	77	107	113	124	107	100	92	103	78	52	24	1746
600	8	3	42	80	123	138	106	128	99	69	60	69	58	30	1227
600	9	7	32	94	109	109	120	87	138	81	82	68	67	13	914

[a] For all the data except at $E_n=270$ kev, the intervals are in the center-of-mass system. The data at 270 kev are grouped in the corresponding intervals in the laboratory system. The total sum of P^{-1} from 0° to 180° is adjusted to 1000 for convenience in comparing the data of the different observers.
[b] Data from glycerine treated plates.

thermal neutrons; it was found to be spherically symmetric, as it should be.

If the s and p components of the incident neutron wave are contributing to the reaction, the angular distribution giving the relative triton yield per unit solid angle will be of the form:

$$Y(E_n, \phi_0)=A'+B' \cos\phi_0+C' \cos^2\phi_0, \quad (2)$$

where A', B', and C' are constants for a given E_n. If we write $Y(E_n, \phi_0)=dN/d\Omega$, where dN is the number of tritons between Ω and $\Omega+d\Omega(d\Omega=2\pi \sin\phi_0 d\phi_0)$, and integrate between the limits ϕ_{01} and ϕ_{02}, we have

$$\frac{1}{2\pi}\int_{\phi_{01}}^{\phi_{02}} dN=\left[A' \cos\phi_0+\frac{B'}{2}\cos^2\phi_0+\frac{C'}{3}\cos^3\phi_0\right]_{\phi_{02}}^{\phi_{01}}. \quad (3)$$

If the data in Table II are divided into three equal ϕ_0 intervals, three simultaneous equations are obtained to evaluate A', B', and C' above for each E_n. If we normalize $\int_0^{4\pi} Y(E_n, \phi_0)d\Omega$ to the total capture cross section as measured by Blair and Holland,[8] we obtain directly the differential cross section $d\sigma(E_n, \phi_0)/d\Omega=A+B \cos\phi_0+C \cos^2\phi_0$. The values of A, B, and C thus determined from the data of each observer are shown in Table I. The statistical accuracy of these coefficients is of the order of 12 percent for the A's and B's, and 20 percent for the C's. The agreement is seen to be reasonably satisfactory in most cases. A series of the type given in Eq. (2) fits the data from the glycerine treated plates more smoothly than it does the data from untreated plates, except for $E_n=270$ kev, where excellent agreement was obtained throughout. Furthermore the data from the glycerine-treated plates were obtained after the observers had acquired more experience. They were therefore arbitrarily given twice as much weight as the data from untreated plates in determining the average value of the coefficients given in Table III. The statistical accuracy of these average coefficients is better than 10 percent for the A's and B's and 15 percent for the C's. A plot of $Y=A+B \cos\phi_0+C \cos^2\phi_0$ using the values of A, B, and C in Table III is shown in Fig. 8.

TABLE III. Average value of the coefficients of the differential cross section of $Li^6(n,\alpha)$.

E_n kev	Coefficients (barns/steradian) A	B	C
200	0.096	0.105	0.215
270	0.17	0.063	0.22
400	0.064	0.043	0.095
600	0.031	0.0095	0.026

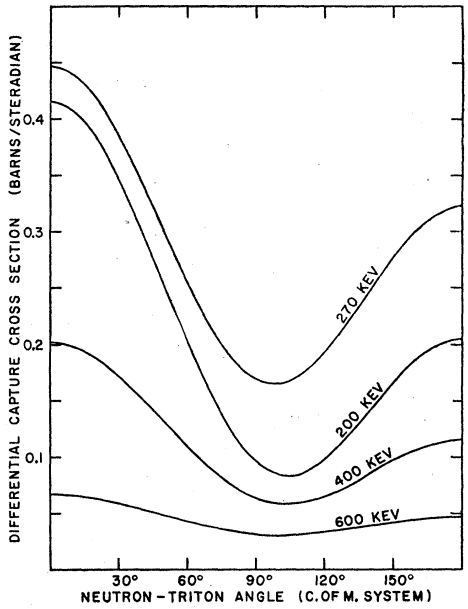

FIG. 8. The differential cross section of $Li^6(n,\alpha)H^3$ for $E_n=200$, 270, 400, and 600 kev. The curves are plotted by using the average coefficients given in Table III.

Measurements of $d\sigma/d\Omega$ for $E_n=100$, 1100, 1500, and 2000 kev are now in progress and will be published later. It is planned also to check some of the measurements with plates loaded with specks of lithium glass. The latter measurements should yield improved accuracy, since the visible specks of glass should make possible a more unique determination of the point of disintegration.

The authors wish to thank Franklin Peterson, Kate Rymer, Margaret Steele, and Elizabeth Stephenson for their patience in measuring most of the tracks and for helping with some of the calculations. We also wish to thank Hubert Billington for developing the plates. Appreciation is also expressed to Alexander Langsdorf and his group at the Argonne Laboratory for valuable assistance in exposing the plates and for the use of their electrostatic generator.

[8] J. M. Blair and R. E. Holland, data reproduced in *Neutron Cross Sections*, Atomic Energy Commission Report 2040 (Office of Technical Services, Washington, D. C., 1952).